

# Topology and manipulation of multiferroic hybrid domains in $\text{MnWO}_4$

D. Meier, N. Leo, M. Maringer, Th. Lottermoser, and M. Fiebig  
*Helmholtz-Institut für Strahlen- und Kernphysik, Universität Bonn*  
*Nussallee 14 - 16, 53115 Bonn, Germany*

P. Becker and L. Bohatý  
*Institut für Kristallographie, Universität zu Köln*  
*Zùlpicher Strasse 49b, 50937 Köln, Germany*  
 (Dated: February 13, 2022)

An investigation of the spatially resolved distribution of domains in the multiferroic phase of  $\text{MnWO}_4$  reveals that characteristic features of magnetic and ferroelectric domains are inseparably entangled. Consequently, the concept of *multiferroic hybrid domains* is introduced for compounds in which ferroelectricity is induced by magnetic order. The three-dimensional structure of the domains is resolved. Annealing cycles reveal a topological memory effect that goes beyond previously reported memory effects and allows one to reconstruct the entire multiferroic multidomain structure subsequent to quenching it.

In the field of strongly correlated electron systems materials with cross-correlated magnetic and electric properties, called magnetoelectrics, are intensely discussed because of their potential for controlling magnetic properties by an electric voltage. Among them, the magnetoelectric multiferroics may be most prominent because due to a coexistence of magnetic and electric order they can develop particularly pronounced magnetoelectric interactions.[1, 2] Recently it was demonstrated that intrinsically strong (“giant”) magnetoelectric effects are present in the so-called joint-order-parameter multiferroics in which magnetic long-range order breaks the inversion symmetry and induces a spontaneous polarization.[3, 4, 5] For example, in  $\text{TbMnO}_3$ ,  $\text{Ni}_3\text{V}_2\text{O}_8$ , and  $\text{MnWO}_4$ , a spiral arrangement of spins violates the inversion symmetry and causes a spontaneous polarization

$$\mathbf{P} \propto \mathbf{e}_{ij} \times (\mathbf{S}_i \times \mathbf{S}_j), \quad (1)$$

with  $\mathbf{e}_{ij}$  as unit vector connecting neighboring spins at sites  $i$  and  $j$  and  $(\mathbf{S}_i \times \mathbf{S}_j)$  as vector chirality.[6, 7, 8] The magnitude and direction of  $\mathbf{P}$  are determined by the magnetic order only, so that a unique correlation between the magnetic and ferroelectric (FEL) order parameters is obtained. Although the spontaneous polarization is usually small, its robustness[9] renders joint-order-parameter multiferroics interesting for future applications.

An essential feature of any ferroic material is the presence of domains. They determine the switching of information bits in memory devices and the technological performance of permanent magnets. At its root, any magnetoelectric interaction in a multiferroic corresponds to an interaction of its magnetic and electric domains. Hence, understanding giant magnetoelectric effects means understanding the nature and interactions of the multidomain state in the joint-order-parameter multiferroics.[16] However, although domains are known to be present in these compounds by a variety of (mostly indirect) experiments[9, 10, 11, 12, 13, 14, 15] the prime target of previous investigations was actually to *remove*

these domains by converting the samples to or in between single-domain states.

Therefore, none of the existing publications addresses the three-dimensional distribution of domains in a joint-order-parameter multiferroic and the effects guiding their formation. With this, essential questions regarding the nature of the domains remain unclear. For example, to what extent can a domain actually be called ferroelectric if the spontaneous polarization is magnetically induced?

In this report, the three-dimensional topology of domains in the joint-order-parameter multiferroic  $\text{MnWO}_4$  is resolved by optical second harmonic generation (SHG). The spatial distribution of the domains, their response to external fields, and annealing procedures reveal some features that are uniquely associated to a magnetic domain state and others that point unambiguously to ferroelectric domains. The concept of “multiferroic hybrid domains” is thus introduced whereas a description in terms of “magnetic domains” or “electric domains” or even “magnetic domains coexisting with electric domains” is no longer appropriate.

The evolution of the multiferroic phases and their domains in joint-order-parameter compounds can be described by Landau theory. In the case of spin-spiral systems it was shown that a coexistence of two magnetic order parameters is required for obtaining multiferroicity.[17, 18, 19, 20] The first magnetic order parameter generally guides the system into a phase with an incommensurate non-polar spin arrangement. Upon cooling another magnetic transition described by a second magnetic order parameter evolves, so that the combination of both breaks the inversion symmetry of the crystal. As a consequence, a spontaneous polarization according to Eq. (1) can emerge.

For the investigation of the local structure of domains in spin-spiral ferroelectrics the choice of  $\text{MnWO}_4$  as a model system suggests itself. On the one hand, its magnetic lattice is rather simple, because no rare-earth and just one kind of transition-metal ion contributes to the magnetic order. On the other hand, the rich magnetic

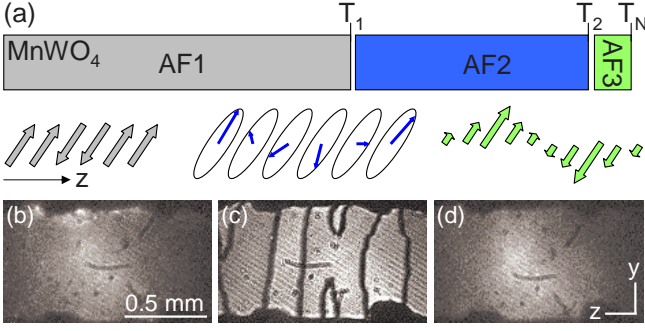


FIG. 1: (a) Magnetic phase transitions in  $\text{MnWO}_4$ . Below the Néel temperature  $T_N$  the  $\text{Mn}^{3+}$  moments display collinear incommensurate long-range order within the easy plane. At  $T_2$  an additional transverse spin component orders which leads to a helical incommensurate arrangement of spins. In the magnetic ground state below  $T_1$  a commensurate up-up-down-down spin ordering is obtained. The spin spiral in the AF2 phase induces a spontaneous electric polarization along the  $y$  axis while the AF1 and AF3 phases are not multiferroic. (b – d) Spatially resolved SHG measurements in the AF1 to AF3 phases. A domain structure (with black lines revealing domain walls) is detected in the multiferroic AF2 phase only.  $x$ ,  $y$ , and  $z$  represent a Cartesian coordinate system, approximating the monoclinic unit cell with lattice parameters  $a = 4.83 \text{ \AA}$ ,  $b = 5.76 \text{ \AA}$ ,  $c = 4.99 \text{ \AA}$  and  $\beta = 91.1^\circ \approx 90^\circ$ .

phase diagram includes transitions from the multiferroic phase to neighboring ordered or disordered states which allows one to probe memory effects in either.[8, 21]

Three magnetically ordered phases determine the low temperature behavior of  $\text{MnWO}_4$ . In the AF3 phase right below  $T_N = 13.5 \text{ K}$  incommensurate antiferromagnetic (AFM) ordering of the  $\text{Mn}^{3+}$  moments described by the order parameter  $\mathcal{O}_{\text{AF3}}$  occurs. The spins align in a collinear way, pointing along the easy-axis within the  $xz$  plane so that they enclose an angle of about  $34^\circ$  with the  $x$  axis of the monoclinic crystal as illustrated in Fig. 1(a). Their magnitude is sinusoidally modulated, leading to a two-dimensional incommensurate spin-density wave with  $\mathbf{k} = (-0.214, \frac{1}{2}, 0.457)$ . [22]

In the multiferroic AF2 phase below  $T_2 = 12.7 \text{ K}$  an additional transverse spin component orders and the spin density wave becomes an elliptical spin spiral while retaining  $\mathbf{k} = (-0.214, \frac{1}{2}, 0.457)$  as wave vector. The related magnetic order parameter  $\mathcal{O}_{\text{AF2}}$  evolves through a second-order phase transition at  $T_2$  and coexists with  $\mathcal{O}_{\text{AF3}}$ . As detailed above, simultaneous presence of the two magnetic order parameters breaks the inversion symmetry and induces a spontaneous polarization, here

$$P_y \propto \mathcal{O}_{\text{AF3}} \mathcal{O}_{\text{AF2}} \quad (2)$$

along to the  $y$  axis, and establishes multiferroicity in  $\text{MnWO}_4$ . Note that  $\mathcal{O}_{\text{AF2}}$  can be reoriented below  $T_2$  while  $\mathcal{O}_{\text{AF3}}$  is frozen.[18, 19, 20] Thus, any reversal of  $\mathcal{O}_{\text{AF2}}$  is coupled one-to-one to a reversal of  $P_y$ . [23, 24]

In the AF1 phase,  $\text{MnWO}_4$  displays collinear commensurate AFM order. The associated wave vector is

$\mathbf{k} = (\pm\frac{1}{4}, \frac{1}{2}, \frac{1}{2})$  and describes an up-up-down-down spin structure with spins aligned along the easy-axis. In agreement with Eq. (1), the magnetic order parameter  $\mathcal{O}_{\text{AF2}}$  and, thus,  $P_y$ , are quenched at the first-order  $\text{AF2} \rightarrow \text{AF1}$  transition at  $T_1 = 7.6 \text{ K}$  while  $\mathcal{O}_{\text{AF3}}$  remains.

Because of the intricate interplay of the order parameters  $\mathcal{O}_{\text{AF2}}$  and  $\mathcal{O}_{\text{AF3}}$  the number and types of domains for the three phases will differ. A powerful technique for investigating domain structures in systems with magnetic or electric order is second harmonic generation (SHG). Optical SHG describes the induction of a light wave at frequency  $2\omega$  by a light wave at frequency  $\omega$ . The process picks up the symmetry changes imposed by the long-range order by coupling directly to the corresponding order parameter and its different orientation in different domains. A detailed discussion of the technical aspects of SHG in ferroic systems in general[25] and in  $\text{MnWO}_4$  in particular[12] was already published so that we restrict ourselves here to the application of SHG for imaging the domain structure of  $\text{MnWO}_4$ .

Obviously, SHG contributions arising at  $T_N$  probe the magnetic order parameter  $\mathcal{O}_{\text{AF3}}$ , while those emerging at  $T_2$  involve coupling to  $\mathcal{O}_{\text{AF2}}$  and, because of Eq. (2), to  $P_y$ . As overview, Figs. 1(b)-(d) show spatially resolved measurements of the SHG intensity in the AF1, AF2, and AF3 phase, respectively. While the AF1 and the AF3 phases reveal a homogeneous distribution of SHG intensity, the multiferroic AF2 phase exhibits about ten curved black lines on an otherwise homogeneous background. Such lines are a hallmark for the presence of domains with opposite orientation of the corresponding order parameter. Because of the linear coupling to the order parameter, the SHG light field experiences a sign reversal corresponding to a  $180^\circ$  phase shift when crossing the domain wall. This leads to destructive interference in the vicinity of the domain wall and, therefore, to the black lines. According to Fig. 1 such  $180^\circ$  domains are present in the multiferroic AF2 phase only while being absent in the AF1 and AF3 phases.

In order to understand this observation we have to analyze the symmetry of the AF1 to AF3 phases. The monoclinic paraelectric and paramagnetic phase of  $\text{MnWO}_4$  belongs to the point-group  $2_y/m_y1'$ . This point symmetry is preserved by the commensurate up-up-down-down spin configuration in the AF1 phase and also by the incommensurate spin-density wave in the AF3 phase because the magnetic order breaks translation symmetries only.[22] Therefore, a formation of domains with different orientation of the order parameter should indeed not occur.[26] In contrast, the multiferroic AF2 phase possesses the point symmetry  $2_y1'$  with half the number of point-symmetry operations as in the group  $2_y/m_y1'$ . As observed, this leads to two domains with an opposite sign of the magnetic order parameter  $\mathcal{O}_{\text{AF2}}$  corresponding to an opposite magnetic vector chirality and, via Eq. (2), to an opposite sign of the spontaneous polarization  $P_y$ .

In the following, we will focus on the discussion of the

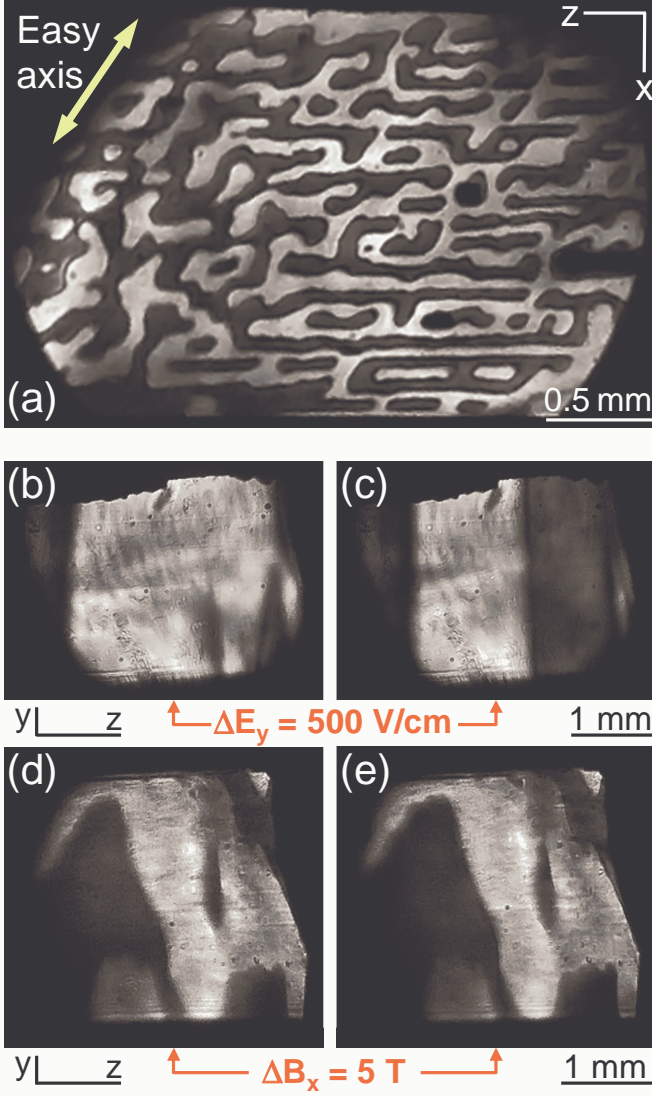


FIG. 2: Spatially resolved SHG images reveal the hybrid nature of the multiferroic domains in  $\text{MnWO}_4$ . (a) Domain structure in the  $xz$  plane. A pronounced elongation along the magnetic easy axis of the crystal (yellow arrow) and the bubble topology reflect the magnetic aspect of the domains. (b, c) Domain structure in electric fields of (b) 167 kV/cm and (c) 217 kV/cm applied along the  $y$  axis. (d, e) Domain structure in magnetic fields of (d) 0 T and (e) 5 T applied along the  $x$  axis. Only the electric field affects the distribution of the domains, thus reflecting their electric aspect.

180° domains in the multiferroic AF2 phase. First of all, we will investigate the topology of the AF2 domains and their response to external poling fields. Figure 2(a) shows the distribution of the AF2 domains in the  $xz$  plane after zero-field cooling. We find a labyrinth-like arrangement of dark and bright areas, being distributed with approximately equal proportions across the sample. The different level of brightness corresponds to opposite magnetic vector chirality and spontaneous polarization according to Eq. (1). In contrast to Fig. 1(c) a different brightness

between opposite domains (in addition to the mere domain walls) is observed because of the interference of the SHG light field arising from the multiferroic order with a homogeneous SHG light field generated by the crystal lattice.[25] The topology of the domains in Fig. 1(a) reveals two preferential directions: along the  $z$  axis and along a line including an angle of about 34° with the  $x$  axis.

Figure 2(a) clearly expresses the magnetic origin of the domain structure. First, the texture of the domains strikingly resembles the patterns of bubble and stripe domains, universally attributed to modulated phases with a preselected equilibrium periodicity.[27] In  $\text{MnWO}_4$  it is the long-range magnetic interaction that stabilizes the modulated AF2 phase and the periodicity is determined by the magnetic wave vector  $\mathbf{k}$ . Second, the preferential direction of the domain walls parallel to the arrow in Fig. 2(a) is in striking coincidence with the direction of the magnetic easy-axis of  $\text{MnWO}_4$  which encloses an angle of 34° – 37° with the  $x$  axis in the  $xz$  plane.[22]

In Figs. 2(b – e) the response of the domain structure in the  $yz$  plane to electric and magnetic fields is shown. It is obvious that with an electric field applied along the  $y$  axis small changes in the order of 1 kV/cm lead to pronounced changes in the topology of the AF2 domains. In contrast, a magnetic field of up to 5 T applied along the  $x$  axis does not alter the domain structure at all [Fig. 2(d) and 2(e)], and the same holds for fields applied along the  $y$  or  $z$  axis. Figures 2(b – e) thus emphasize the electric nature of the AF2 domain structure.

We therefore conclude that the AF2 domains exhibits hallmarks of both a magnetically *and* an electrically ordered state. The *topology* is determined by the *magnetic* character of the domains, whereas the *field response* reflects the *electric* character. Because of this bilateral nature, only a denomination of the AF2 domains as *multiferroic hybrid domains* seems appropriate whereas a description in terms of ferroelectric or antiferromagnetic remains incomplete. This is in stark contrast to earlier work[12] where magnetic and ferroelectric domains were still considered as strictly separate entities. It was already pointed out that the improper nature of the ferroelectric polarization implies rigid coupling to the magnetic order parameters.[23, 24] However, this seems to be the first work where the consequences of this relation on the level of the domain structure is revealed. Only this leads to the realization that an extended concept of multiferroic hybrid domains is required.

The full three-dimensional topology of the multiferroic domains is presented in Fig. 3 for three differently oriented  $\text{MnWO}_4$  samples obtained from the same batch. Figure 3(a) shows the domain structure in the  $xz$  plane. Like in Fig. 2(a), dark and bright regions correspond to the two possible multiferroic domains with opposite order parameters. We can see the aforementioned elongation of domains along the magnetic easy-axis with the spontaneous polarization  $P_y$  pointing into and out of the plane. The propagation of domain walls along the direction of



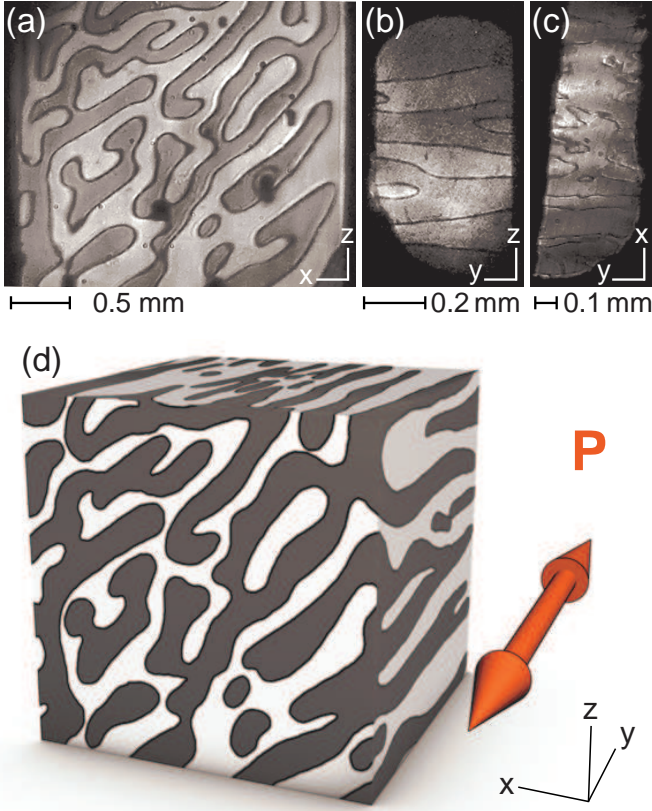


FIG. 3: Three-dimensional distribution of the multiferroic domains. (a – c) Domains in the  $xz$ ,  $yz$ , and  $xy$  plane of  $\text{MnWO}_4$  samples taken from the same batch. (d) Three-dimensional visualization of the multiferroic domain structure in (a – c).

the spontaneous polarization is revealed by Figs. 3(b) and 3(c). Interestingly, the domain walls, here again indicated by the black lines, continue rather straight along the  $y$  axis of the crystal. The domains tend to form platelets in planes defined by the magnetic easy-axis and the direction of the spontaneous polarization. With a lateral extension evaluated as  $170 \pm 60 \mu\text{m}$ [28] the domains are surprisingly large. For an improved visualization of the anisotropic multiferroic domain structure, Fig. 3(d) shows a three-dimensional simulation based on the distribution of domains in Figs. 3(a – c). The respective domain structure were projected onto three faces of a cuboid and mended minimally at the edges.

In the following we consider the dynamic aspects in the formation of the domains by applying annealing procedures across the boundaries limiting the multiferroic phase. First of all, we consider the effect of temperature-annealing in an order  $\leftrightarrow$  disorder cycle from the AF2 phase to the paramagnetic state above  $T_N$  and back to the multiferroic phase. Initially, the sample was zero-field-cooled from room temperature into the AF2 phase which leads to the SHG image shown in Fig. 4(a). In agreement with Fig. 1, a multiplicity of domains is obtained. Subsequently, the order  $\leftrightarrow$  disorder annealing

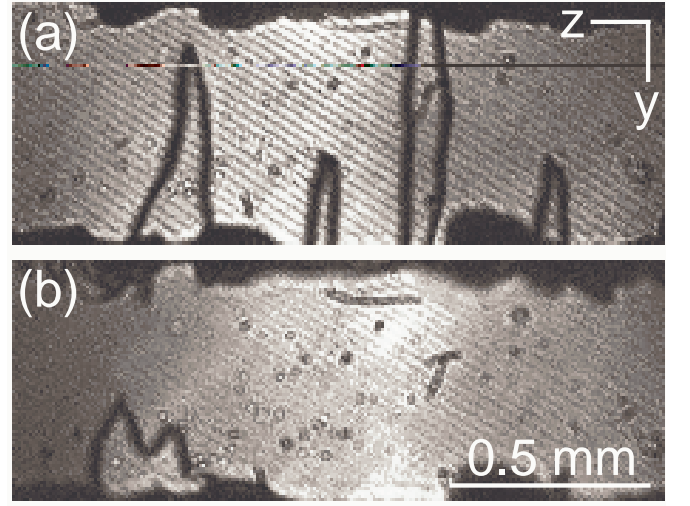


FIG. 4: Response of the multiferroic domains to a temperature annealing cycle through the paramagnetic phase. (a) Domain structure after initial zero-field cooling from room temperature to the multiferroic AF2 phase. (b) Domain structure after subsequent application of the annealing cycle.

cycle was applied which leads to the SHG image shown in Fig. 4(b). Most of the domain walls have vanished and only a small fraction of the  $\text{MnWO}_4$  remains in a domain state opposite to the rest of the sample. Apparently, the annealing procedure tends to drive the sample towards a single domain state which was confirmed by repeating the experiment more than ten times.

Figure 4 leads to two conclusions. First, no memory effect is observed in the order  $\leftrightarrow$  disorder annealing cycle. Second, while conventional ferroelectrics tend to form a multiplicity of domains for minimizing electric stray fields, an ideal antiferromagnet tends to approach a single-domain state.[29] Hence, just like the domain structure itself (Fig. 2) the dynamic domain topology is dominated by the magnetic aspect of the hybrid multiferroic order.

In the second step, we investigated the effect of an order  $\leftrightarrow$  order annealing cycle from the AF2 phase to the AF1 phase and back to the multiferroic state. This transition is of particular interest because of a FEL memory effect reported earlier:[21, 30] A single-domain state in the multiferroic phase is memorized in the non-polar AF1 phase and reemerges when reentering the AF2 phase. However, all current data were gained by integral techniques such as pyroelectric current measurements, so that it is not known to what extent the memory effect applies to the domain structure of the multiferroic multidomain state.

This is investigated in Fig. 5 which compares the domain structure of the AF2 phase before [panels (b), (d)] and after [panels (c), (e)] the annealing cycle through the AF1 phase. Figure 5(a) illustrates that the phase boundary between the AF2 and the AF1 phase can be crossed by magnetic-field or temperature tuning. Figures 5(b)

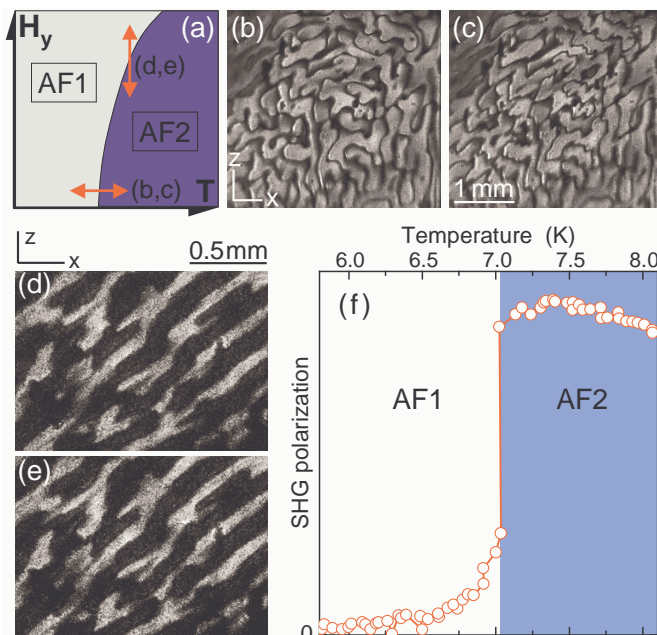


FIG. 5: Response of the multiferroic domains to magnetic-field ( $H$ ) and temperature ( $T$ ) annealing cycles through the AF1 phase. (a) Sketch of the ( $H, T$ ) phase diagram with arrows indicating the respective annealing procedure. (b, d) Domain structure after initial zero-field cooling from room temperature to the multiferroic AF2 phase. (c, e) Domain structure after application of the respective annealing cycle. (f) Temperature dependence of the SHG signal ( $\chi_{yxx}$  component at 1.95 eV)[12] in a temperature decreasing run. Nonzero SHG yield in the AF1 phase points to a residual polar contribution in the AF1 phase as probable basis of the topological memory effect revealed in panels (b – e).

and 5(c) reveal the effects of thermal annealing. Minor changes in the roughness of the domain walls and, for a small fraction of the walls, shifts in the order of 100  $\mu\text{m}$  are observed but the general distribution of the domains is preserved. Annealing in a magnetic field along the  $y$  axis reveals no changes at all in the domain structure. Hence, not only a single-domain state is memorized in the non-chiral non-polar AF1 phase — actually the entire topology of a multidomain state is preserved. The memory effect is thus much more rigid than established up to now.

Figure 5 immediately raises the question for the origin of such a memory effect. Pinning of the domain structure by structural defects can be excluded. This mechanism would also preserve the domain structure in the order  $\leftrightarrow$  disorder transition to the paramagnetic phase contrary to what Fig. 4 shows. For revealing its origin we measured the temperature dependence of the magnetic order parameter  $\mathcal{O}_{AF2}$  across the AF2  $\rightarrow$  AF1 transition. As

shown in Fig 5(f), the SHG contribution that is related to the magnetic order parameter  $\mathcal{O}_{AF2}$  does not vanish abruptly at the phase boundary to the AF1 state. Instead, it diminishes gradually with temperature after an initial step-like decrease. The remanent SHG signal reveals a coexistence of the AF1 and AF2 phase within a broad temperature region, enabled by the first-order nature of the transition. Hence, residual nuclei of the AF2 phase explain the “polar memory” of  $\text{MnWO}_4$ . [30] The distribution of the nuclei must be homogeneous and dense in order to explain pinning of the entire topology of a multidomain state. Note that 5(f) is the first measurement directly proving the existence of polar inclusions within the AF1 phase, which is possible because of the extraordinary sensitivity of SHG to nanoscopic inclusions.[31]

In summary, we revealed that the magnetically induced ferroelectric phase of the joint-order-parameter multiferroic  $\text{MnWO}_4$  forms novel types of domains for which characteristic features of magnetic and ferroelectric domains are inseparably entangled. Here the denomination as *multiferroic hybrid domain* is introduced. In  $\text{MnWO}_4$  the *topology* of these chimera domains is determined by their *magnetic* nature, whereas the *field response* reflects the *electric* character. The three-dimensional distribution of the domains was investigated and annealing cycles revealed a topological memory effect allowing one to reconstruct the entire multidomain structure subsequent to quenching it.

The present work should provide a basis for the development of a model explaining the topology of domains in compounds with magnetically induced ferroelectricity. Regarding long-term application, a vastly increasing variety of joint-order-parameter multiferroics allowing ferroelectricity according to Eq. (2) are at our disposal for multiferroic domain control. The discovery of mechanisms promoting magnetically induced ferroelectricity different from Eq. (2) is only a question of time and may eventually lead us towards high-temperature applications. Because of the bilateral nature of the multiferroic hybrid domains systems with conical spin spirals allow one to exert rigid electric-field control of a macroscopic magnetization.[23] Since magnetization and polarization are manifestations of the same multiferroic hybrid domain state the electric field will always act on both. Rapid magnetization reversal with ultrashort electric-field pulses may thus become feasible.

## Acknowledgments

We thank Steffen Brosseit and BrossBoss Entertainment for designing the 3D domain structure. This work was supported by the DFG through the SFB608.

[1] W. Eerenstein, N. D. Mathur, and J. F. Scott, Nature (London) **442**, 759 (2006).

[2] S.-W. Cheong and M. Mostovoy, Nature Mater. **6**, 13

- (2007).
- [3] R. E. Newnham, J. J. Kramer, W. A. Schulze, and L. E. Cross, *J. Appl. Phys.* **49**, 6088 (1978).
  - [4] T. Kimura, T. Goto, H. Shintani, I. K., T. Arima, and Y. Tokura, *Nature (London)* **426**, 55 (2003).
  - [5] N. Hur, S. Park, P. A. Sharma, J. S. Ahn, S. Guha, and S.-W. Cheong, *Nature (London)* **429**, 392 (2004).
  - [6] M. Kenzelmann, A. B. Harris, S. Jonas, C. Broholm, J. Schefer, S. B. Kim, C. L. Zhang, S.-W. Cheong, O. P. Vajk, and J. W. Lynn, *Phys. Rev. Lett.* **95**, 087206 (2005).
  - [7] G. Lawes, A. B. Harris, T. Kimura, N. Rogado, R. J. Cava, A. Aharony, O. Entin-Wohlman, T. Yildirim, M. Kenzelmann, C. Broholm, et al., *Phys. Rev. Lett.* **95**, 087205 (2005).
  - [8] K. Taniguchi, N. Abe, T. Takenobu, Y. Iwasa, and T. Arima, *Phys. Rev. Lett.* **97**, 097203 (2006).
  - [9] T. Kimura, Y. Sekio, H. Nakamura, T. Siegrist, and A. P. Ramirez, *Nature Mater.* **7**, 291 (2008).
  - [10] Y. J. Choi, J. Okamoto, D. J. Huang, K. S. Chao, H. J. Lin, C. T. Chen, M. van Veenendaal, T. A. Kaplan, and S.-W. Cheong, *Phys. Rev. Lett.* **102**, 067601 (2009).
  - [11] Y. Bodenthin, U. Staub, M. Garcia-Fernandez, M. Janoschek, J. Schlappa, E. I. Golovenchits, V. A. Sanina, and S. G. Lushnikov, *Phys. Rev. Lett.* **100**, 027201 (2008).
  - [12] D. Meier, M. Maringer, T. Lottermoser, P. Becker, L. Bohatý, and M. Fiebig, *Phys. Rev. Lett.* **102**, 107202 (2009).
  - [13] B. Kundys, C. Simon, and C. Martin, *Phys. Rev. B* **77**, 172402 (2008).
  - [14] P. G. Radaelli, L. C. Chapon, A. Daoud-Aladine, C. Vecchini, P. J. Brown, T. Chatterji, S. Park, and S.-W. Cheong, *Phys. Rev. Lett.* **101**, 067205 (2008).
  - [15] I. Cabrera, M. Kenzelmann, G. Lawes, Y. Chen, W. C. Chen, R. Erwin, T. R. Gentile, J. B. Leao, J. W. Lynn, N. Rogado, et al., *cond-mat* **0904.2603v1**, 0904.2603v1 (2009).
  - [16] A. Loidl, H. von Loehneysen, and G. M. Kalvius, *J. Phys.: Condens. Matter* **20**, 430301 (2008).
  - [17] P. Tolédano, W. Schranz, and G. Krenner, *Phys. Rev. B* **79**, 144103 (2009).
  - [18] P. Tolédano, *Phys. Rev. B* **79**, 094416 (2009).
  - [19] A. B. Harris, *Phys. Rev. B* **76**, 054447 (2007).
  - [20] G. Lawes, M. Kenzelmann, and Broholm, *J. Phys.: Cond. Mat.* **20**, 434205 (2008).
  - [21] A. H. Arkenbout, T. T. M. Palstra, T. Siegrist, and T. Kimura, *Phys. Rev. B* **74**, 184431 (2006).
  - [22] G. Lautenschläger, H. Weitzel, T. Vogt, R. Hock, A. Böhm, M. Bonnet, and H. Fuess, *Phys. Rev. B* **48**, 6087 (1993).
  - [23] Y. Yamasaki, S. Miyasaka, Y. Kaneko, J.-P. He, T. Arima, and Y. Tokura, *Phys. Rev. Lett.* **96**, 207204 (2006).
  - [24] Y. Tokunaga, N. Furukawa, H. Sakai, Y. Taguchi, T. Arima, and Y. Tokura, *Nature Mater.* **8**, 558 (2009).
  - [25] M. Fiebig, V. V. Pavlov, and R. V. Pisarev, *J. Opt. Soc. Am. B* **22**, 96 (2005).
  - [26] Antiphase domains, also called translation domains, may occur.[12] However, they result from the violation of only the translation symmetry and do not differ in the orientation of the order parameter. Therefore, they are not considered henceforth.
  - [27] M. Seul and D. Andelman, *Science* **267**, 476 (1995).
  - [28] A. Hubert and R. Schäfer, *Magnetic domains: The Analysis of Magnetic Microstructures* (Springer, Berlin, 1998).
  - [29] Y. Y. Li, *Phys. Rev.* **101**, 1450 (1956).
  - [30] K. Taniguchi, N. Abe, S. Ohtani, and T. Arima, *Phys. Rev. Lett.* **102**, 147201 (2009).
  - [31] T. Kordel, C. Wehrenfennig, D. Meier, T. Lottermoser, M. Fiebig, I. Gélard, C. Dubourdieu, J.-W. Kim, L. Schultz, and K. Dörr, *Phys. Rev. B* **80**, 045409 (2009).